A STRESS-TOLERANT TEMPERATURE-STABLE RF MEMS SWITCHED CAPACITOR

I. Reines[1], B. Pillans[2], and G.M. Rebeiz[1]
[1]University of California San Diego, La Jolla, California, USA
[2]Raytheon Systems Co. Dallas, Texas, USA

ABSTRACT

We present the design, fabrication, and measurement of an RF MEMS (Radio Frequency Micro-Electromechanical System) switched capacitor that exhibits reduced sensitivity to residual stress and temperature. The device is based on a circularly symmetric geometry with arc-type springs placed between the anchors and suspended beam. This design compensates for the effects of the residual biaxial stress in the beam, resulting in a pull-in voltage slope versus temperature of only -50 mV/ ºC from -5 ºC to 95 ºC. Reducing the device sensitivity to residual stress improves the performance uniformity on a wafer-scale, and from wafer-to-wafer lots.

1. INTRODUCTION

RF MEMS switched capacitors offer key advantages in terms of linearity, loss, and power consumption compared to conventional solid-state switches [1]. To date, they have been used extensively in a wide range of RF switching and reconfigurable networks with excellent performance [2-3]. One drawback of commonly used fixed-fixed beam capacitive RF MEMS switches is their sensitivity to residual bi-axial stress. This limits the operating temperature, leads to excessively varying actuation voltage and up-state capacitance versus temperature, and reduces the power handling and device uniformity [4-6]. The device performance varies with temperature because a large portion of the spring constant is dependent on the residual stress, which changes with temperature due to the coefficient of thermal expansion (CTE) mismatch between the substrate and bridge. H. Nieminen previously reported a temperature-stable RF MEM capacitor whose design necessitated 4-10 µm thick spring metal to reduce initial beam displacement from a stress gradient [7].

The circular beam geometry presented here can be designed with the appropriate stiffness within a thin beam metal process (t_{beam} < 1 µm) while maintaining excellent electrical and mechanical performance over a wide temperature range. The symmetry of the design also reduces the sensitivity to vertical stress gradients and therefore minimizes the initial displacement of the suspended beam.

2. SWITCH DESIGN

Mechanical Properties

The spring constant of fixed-fixed beams is given by $k_{total} = k_1+k_2$, where the k_1 portion is due to the stiffness of the bridge which is determined by material characteristics such as Young's modulus and the moment of inertia. The k_2 portion is due to residual biaxial stress in the beam and is controlled by the fabrication process. A symmetric circular geometry has been investigated to try and minimize the contribution of k_2 relative to k_1. This will decrease the variation in beam stiffness versus residual stress and temperature. In general, this is easier for thicker beam metals since $k_1 \sim t^3$ and $k_2 \sim t$.

The top view and cross section of the CPW implemented shunt switched capacitor are presented in Fig.1. The suspended plate is anchored symmetrically in four locations with arc-angled cutouts placed next to each anchor that define the springs that function to reduce k_2. The device is actuated by supplying a DC voltage between the ground and signal electrodes.

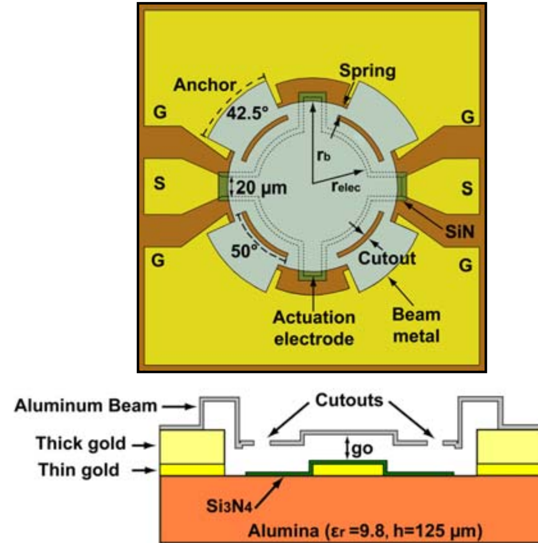

Figure 1: Circular MEMS switched capacitor, (top) layout, (bottom) cross-section.

The switched capacitor was designed to result in an up-state capacitance of 55 fF and a down-state capacitance of 1.5 pF (C_r = 27), given fixed process parameters. Electro-mechanical simulations of this structure were performed using CoventorWare [8], and the mechanical parameters are given in Table 1. The spring constant is defined for a displacement in the center of the beam given a distributed force applied to the top of the membrane over the actuation area.

Table 1: Mechanical parameters of the switched capacitor.

Parameter	Value
Effective area: A (µm^2)	13923
Beam radius: r_b (µm)	97
Electrode radius: r_{elec} (µm)	60
Spring width: w_s (µm)	10
Cutout width: w_c (µm)	5
Beam height: g_o (µm)	3.5
Spring constant[1]: k (N/m)	8.46
Pull-down voltage: V_p (V)	25.9
Resonant frequency[1]: f_o (kHz)	123

[1]simulated using CoventorWare assuming σ_{res} = 60 MPa

In-Plane Stress and Temperature

Mechanical simulations were performed on the circular switched capacitor to investigate the resulting change in the beam stiffness versus average in-plane tensile stress. As shown in Fig. 2, the spring constant increases by only 1.44 N/m for a residual stress of 180 MPa, which results in a maximum k_2/k_1 ratio of 18 %. For comparison, an ideal rectangular beam with dimensions width = 80 µm, length = 145 µm, and t_{beam}= 0.5 µm results in a k_1 portion equal to the circular design (k_1 = 8 N/m) as calculated from [1]. However, a beam stress of 180 MPa will result in a k_2/k_1 ratio of 2064%, demonstrating its sensitivity to in-plane residual stress.

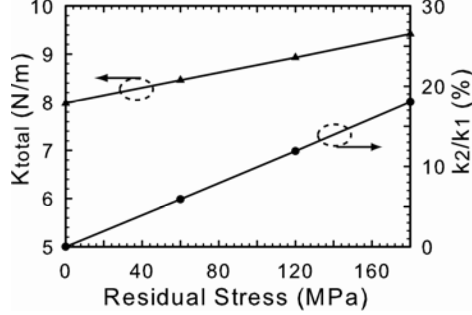

Figure 2: Simulated circular beam stiffness and k_2/k_1 for a varying in-plane residual stress.

When the switch is subjected to a temperature increase ΔT, the fixed anchors will exert a force on the suspended beam which induces a compressive stress, and this reduces the initial residual stress by:

$$\sigma_{total} = \sigma_{residual} - \alpha' E \Delta T \quad (1)$$

$$\alpha' = \alpha_{beam} - \alpha_{substrate} \quad (2)$$

where E is Young's modulus of the beam material, ΔT is the temperature difference, and α' is the CTE mismatch between the substrate and the beam (10-20 ppm/ºC).

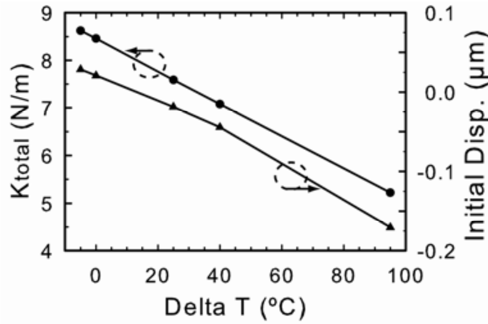

Figure 3: Simulated circular beam stiffness and maximum initial beam displacement (σ_{res} = 60 MPa, $\alpha_{substrate}$= 0 ppm/ºC).

The total spring constant and displacement of the beam were simulated versus ΔT for a residual in–plane tensile stress of 60 MPa, assuming no substrate expansion. As shown in Fig. 3 the spring constant decreases linearly from 8.62 N/m to 5.22 N/m across the 100 ºC range. The displacement is maximum at the center of the plate which deflects downwards by 0.17 µm for ΔT = +95 ºC. This is due to the topography in the circular plate from the underlying bottom electrode and dielectric layers which creates bending moments in the beam that increase displacement versus initial residual stress and temperature, and should therefore be minimized if possible.

Stress Gradients and Temperature

The switched capacitor was also simulated versus varying vertical stress gradients. To approximate a stress gradient in Coventorware, the beam was divided into two equal-thickness layers that were assigned different average in-plane stress values while keeping the total average beam stress fixed at 60 MPa. As shown in Fig. 4, a vertical stress gradient increases both the beam stiffness and ratio of k_2/k_1 compared to an in-plane stress of 60 MPa. Simulations show that a varying stress gradient of 10-50 MPa/µm will result in an initial upward deflection from 0.1 - 0.34 µm.

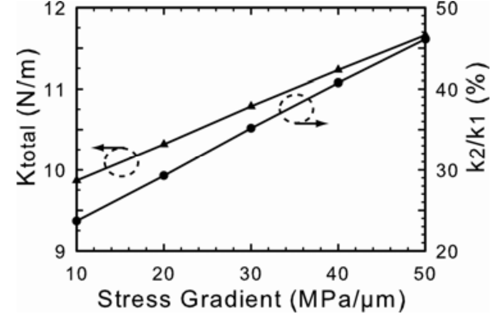

Figure 4: Simulated circular beam stiffness and ratio of k_2/k_1 for a varying vertical stress gradient.

The effects of a 20 MPa/µm stress gradient on beam stiffness and maximum initial displacement were simulated versus ΔT as shown in Fig. 5. The spring constant decreases linearly from 10.46 N/m to 6.48 N/m, while the center of the beam deflects downwards by 0.23 um across this 100 ºC temperature range. Simulations of the circular beam geometry indicate that there is a tradeoff between reduced sensitivity to in-plane stress and initial beam deflection due to a stress gradient. For example, if the cutout angle in the beam is increased, the ratio of k_2/k_1 is reduced for an in-plane stress at the expense of more initial displacement from a stress gradient.

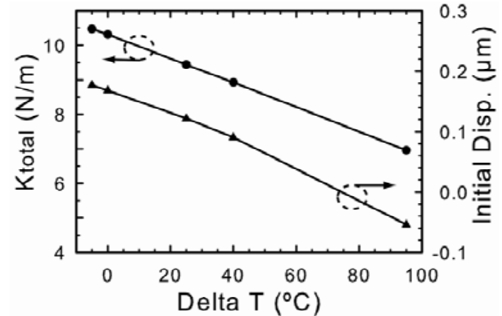

Figure 5: Simulated circular beam stiffness and maximum initial displacement ($\Delta\sigma_{grad}$ = 20 MPa/µm, $\alpha_{substrate}$= 0 ppm/ºC).

3. FABRICATION

The switched capacitor is fabricated on a 125 µm alumina substrate (ε_r = 9.8, tan δ = 0.0001) using an RF MEMS capacitive switch process developed at Raytheon Co. A thin gold layer is first deposited that creates the bottom electrode of the capacitor. A layer of Si_3N_4 is then

deposited on top of the bottom electrode to form the dielectric. A thick gold layer is used as support posts for the suspended beam and to reduce conductor losses in the transmission lines. Next a thin aluminum beam metal is deposited on top of a sacrificial layer which is later removed with surface micromachining to release the suspended membrane. To accommodate the release process, small circular holes are etched in the beam metal. It should be noted that these holes were not included in the electro-mechanical simulations. Test structures were also not included on this first fabrication run to de-embed the resulting biaxial stress in the fabricated devices but the in-plane stress is typically 60 MPa. A micrograph and 3-D white light interferometer image of the fabricated device are shown in Fig. 6.

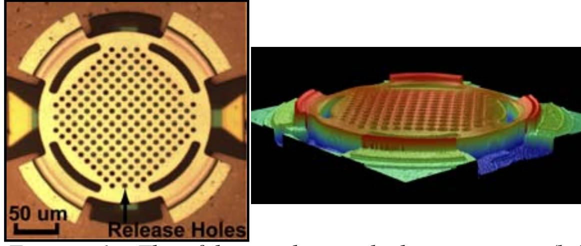

Figure 6: The fabricated switched capacitor, (left) micrograph, (right) 3-D white light interferometer image.

4. MEASUREMENTS

Pull-in Voltage vs. Temperature

The actuation voltage for both circular and standard [5] switched capacitors from two separate wafer lots were measured across a temperature range from -5 ºC to 95 ºC as shown in Fig. 8. The average pull-in voltage slope versus temperature for the two wafers is -50 mV/ ºC for the circular design, compared to -340 mV/ ºC for the standard switch. The spring constants were calculated using the measured actuation voltage and as-released gap heights for the devices from each wafer. The circular switches from wafers 1 and 2 have a k_{total} = 5.05 N/m and 7.84 N/m respectively. After temperature cycling, the circular devices were retested at room temperature and showed no change in actuation voltage or up-state capacitance from initial measurements.

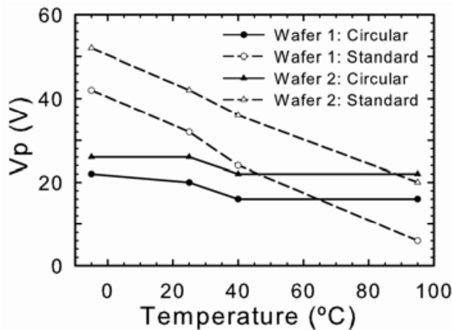

Figure 8: Measured pull-in voltage vs. temperature for both circular and standard switched capacitors from 2 wafer lots.

RF Characterization

The CPW implemented shunt switched capacitor was measured from 0.4 to 30 GHz in both the up-and-down states and versus temperature as shown in Figs.9-10. The up and down-state capacitances were extracted by fitting the measured S-parameters to the lumped element model (Fig. 11). At room temperature, the switch has less than 0.51 dB insertion loss with better than 10 dB return loss up to 30 GHz (the insertion loss is dominated by the reflection coefficient, $1-|\Gamma|^2$). The equivalent up and down-state capacitances are C_u = 64 fF and C_d = 0.89 pF (C_r= 14). The down-state capacitance was reduced due to a rougher-than-normal dielectric. The up-state capacitance from the bridge increases from 53 fF to 58 fF from -5 ºC - 95 ºC as the average gap height decreases by 0.26 μm. The down-state capacitance did not change across the 100 ºC temperature range. The insertion loss of the switch can be reduced in future designs by optimization of the transitions in the CPW line surrounding the switch and resulting in a reduced reflection coefficient up to 30 GHz.

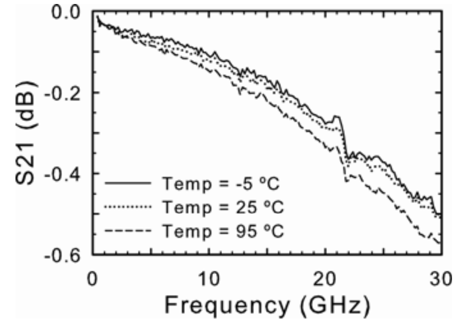

Figure 9: Up-state insertion loss of the switched capacitor from -5 ºC to 95 ºC (C_{bridge}=55.5 fF +/- 2.5 fF).

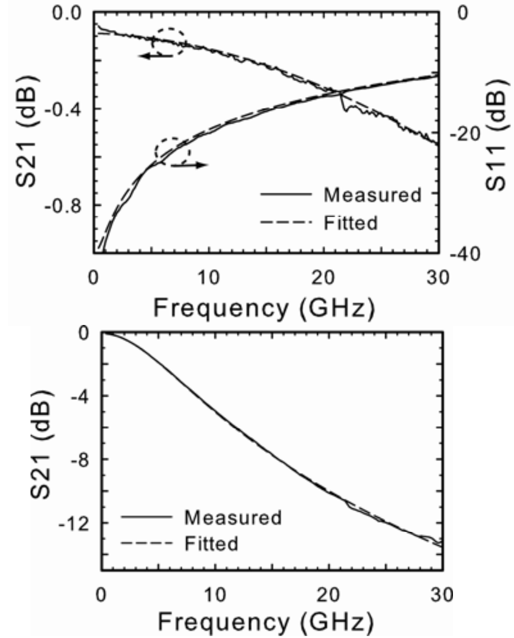

Figure 10: Measured and fitted S-parameters, (top) up-state, (bottom) down-state.

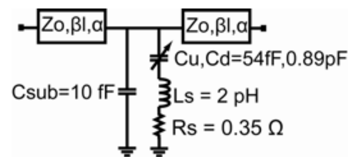

Figure 11: Equivalent lumped- element circuit model

The RF power handling of the switched capacitor was tested under a continuous power at 14 GHz, and the release voltage was measured versus incident power (Fig.

12). The switched circular capacitors from both wafer lots handled 2 W of continuous RF power before latching occurred.

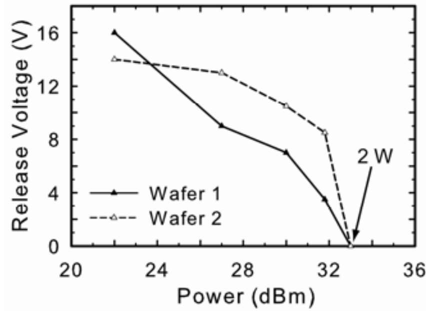

Figure 12: Measured release voltage as a function of continuous RF power at 14 GHz.

Switching Speed & Resonance Frequency

The switching speed measurement setup is depicted in Fig. 13. The switch is actuated at a rate of 100 Hz with a unipolar voltage from 0-40 V, and injected with 10 dBm of incident power at 10 GHz. The modulated output power is monitored with a power detector. The back-to-back waveguide to coax transitions act as a low frequency block to prevent leakage from the stepped voltage into the detector. A switching speed of 8 µs from up-to-down was measured as shown if Fig.13.

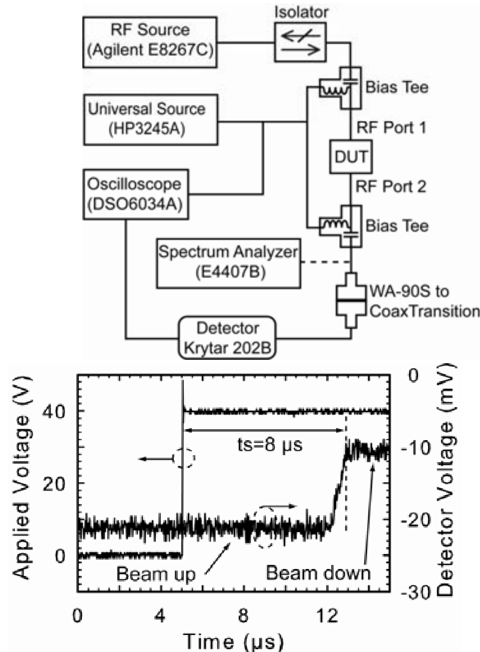

Figure 13: Switching speed and resonance frequency measurement setup (top), and measured switching speed from up-to-down state (bottom).

The mechanical resonance frequency was measured with the setup depicted in Fig. 12. For this measurement the switch is subject to a voltage given by:

$$V_{TOTAL} = V_{DC} + V_{LF}\cos(\omega_{LF}t) + V_{RF}\cos(\omega_{RF}t) \quad (3)$$

where there first two terms are applied from the universal source through the bias tees with $V_{DC} = 10$ V, $V_{LF} = 10$ V, and $f_{LF} = 10 - 200$ kHz. An RF power of 10 dBm at 10 GHz is applied and the modulated output signal from the switch is connected directly to a spectrum analyzer. The resonance frequency is measured by plotting the amplitude of the intermodulation products at f_{RF} +/- f_{LF} while sweeping f_{LF}. The mechanical resonance frequency was measured at 102 kHz with a fitted quality factor of 1.95 as shown in Fig. 14.

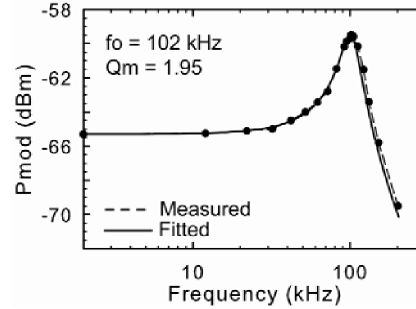

Figure 14: Measured mechanical resonance frequency of the circular switched capacitor.

5. CONCLUSIONS

An RF MEMS switched capacitor has been designed fabricated and tested showing reduced sensitivity to residual bi-axial stress and temperature. This device has a measured pull-in voltage slope versus temperature of only -50 mV/ ºC from -5ºC to 95ºC compared to -340 mV / ºC for standard rectangular devices. Across this temperature range the up-state capacitance varied by only 7.6 % or +/- 2.5 fF. This design improves the uniformity on a wafer-scale and from wafer-to-wafer lots increasing yield and manufacturability. RF measurements verify that this design results in good electrical performance up to 30 GHz over a wide temperature range. This work was supported under the UCSD/DARPA (N/MEMS) Science and Technology Center on RF MEMS.

REFERENCES

[1] G. M. Rebeiz, RF MEMS Theory, Design, and Technology. John Wiley, 2003

[2] C. Nordquist et al. “A DC to 10-GHz 6-b RF MEMS Time Delay Circuit”, *IEEE Microwave and Wireless Component Lett.*, vol. 16, no. 5, pp. 305-307, May 2006.

[3] S. Park et al. “Low-Loss 4-6 GHz Tunable Filter With 3-Bit High-Q Orthogonal Bias RF-MEMS Capacitance Network”, *IEEE Trans. on Microwave. Theory and Tech.*, vol. 56, no. 10, pp. 2348-2355, October, 2008.

[4] C. Goldsmith et al. “Temperature Variation of Actuation Voltage in Capacitive MEMS Switches”, *IEEE Microwave. and Wireless Component Lett.,* vol. 15, no. 10, pp. 718-720, October, 2005.

[5] B. Pillans, “RF MEMS reliability at Raytheon”, in Proc. *IEEE MTT-S Workshop WFF: Reliability Testing & Reliability Enhancement in RF MEMS Switches*, June, 2004.

[6] J. Reid et al. “RF Actuation of Capacitive MEMS Switches”, *IEEE MTT-S*, pp. 1919-1922, June 2003.

[7] H. Nieminen et al. “Design of a Temperature-Stable RF MEM Capacitor”, *J. MEMS*, vol.13, no.5, pp. 705-714, October, 2004.

[8] CoventorWare[tm], http:// www.coventor.com